

# Label Geometry Aware Discriminator for Conditional Generative Networks

Suman Sapkota\*  
NAAMII, Nepal

Bidur Khanal\*  
NAAMII, Nepal

Binod Bhattarai†  
Imperial College London

Bishesh Khanal  
NAAMII, Nepal

Tae-Kyun Kim  
Imperial College London, UK and KAIST, South Korea

## Abstract

*Multi-domain image-to-image translation with conditional Generative Adversarial Networks (GANs) can generate highly photo realistic images with desired target classes, yet these synthetic images have not always been helpful to improve downstream supervised tasks such as image classification. Improving downstream tasks with synthetic examples requires generating images with high fidelity to the unknown conditional distribution of the target class, which many labeled conditional GANs attempt to achieve by adding soft-max cross-entropy loss based auxiliary classifier in the discriminator. As recent studies suggest that the soft-max loss in Euclidean space of deep feature does not leverage their intrinsic angular distribution, we propose to replace this loss in auxiliary classifier with an additive angular margin (AAM) loss that takes benefit of the intrinsic angular distribution, and promotes intra-class compactness and inter-class separation to help generator synthesize high fidelity images.*

*We validate our method on RaFD and CIFAR-100, two challenging face expression and natural image classification data set. Our method outperforms state-of-the-art methods in several different evaluation criteria including recently proposed GAN-train and GAN-test metrics designed to assess the impact of synthetic data on downstream classification task, assessing the usefulness in data augmentation for supervised tasks with prediction accuracy score and average confidence score, and the well known FID metric.*

## 1. Introduction

Image-to-image translation task with conditional Generative Adversarial Networks (cGANs) has seen tremendous progress in recent years, synthesizing realistic images from

input source images conditioned with target styles or domains [20, 54, 32, 8, 17, 22]. Such synthetic images are increasingly being used for augmentation in discriminative tasks for diverse applications including face recognition [10].

Although GANs can generate highly realistic-looking images these days, the high perceptual quality can be deceiving when these images are used for downstream tasks. *Seeing is not believing* [36] and [40] show that using synthetic images for downstream tasks do not necessarily improve their performance even when the quality of the synthetic images seem to match real image distribution qualitatively or under commonly used evaluation metrics like Inception score. In order to better assess the quality of generated images for downstream tasks, [40] propose GAN-train and GAN-test metrics. Some work try to improve the downstream tasks by exploring methods that selectively sample only a subset of generated images [3, 47]. However, a separate sampler adds new set of hyperparameters or computation, and may be less attractive compared to generating better samples in the first place. Generating better samples that can be used for augmentation of downstream task would require greater control over the target class attributes and achieve two important goals: *fidelity* and *coverage*. In other words, synthetic examples for data augmentation should have high fidelity to the target class while preserving the remaining attributes, and be diverse enough following the real conditional data distribution over its full support. This is particularly important in applications such as human face expressions where minor but very specific variation in images results in the image attribute to change to a specific class, e.g. contempt to anger.

Several state-of-the-art labeled conditional GANs for multi-domain image-to-image translation use auxiliary soft-max classifiers [32, 8] in addition to the standard adversarial and reconstruction losses. Table 1 shows the impact of using different weights for auxiliary soft-max classification loss in a popular labeled conditional GAN, StarGAN [8].

\*Equal contribution

†Corresponding author, b.bhattarai@imperial.ac.uk

The result highlights the importance of auxiliary classification loss with the variation in its weight significantly affecting the GAN performance. We propose to improve this auxiliary classification component of labeled conditional GANs helping generator to synthesize better class conditional samples. Inspired from recent progress in discriminative models for classification with the introduction of angular loss with margin [44, 9, 7], we replace the soft-max loss of the auxiliary classifier with the additive angular margin (AAM) loss [9]. This modification helps the auxiliary classifier to learn representation that promote intra-class compactness and inter-class separation, and is better adapted to the intrinsic angular distribution of deep features [7]. Although various forms of angular loss and margins are possible, AAM loss has better geometric attribute with exact correspondence to the geodesic distance and perform better in supervised classification tasks [9]. We hypothesize that these properties of the AAM loss are helpful in cGAN training as well, encouraging generator to improve the fidelity and coverage to the the class conditional distribution. Moreover, as part of the AAM loss computation, we normalize the weights of the classifier to project it into a unit hypersphere which naturally lends itself to the stability of GAN training with bounded discriminator [13, 30, 33]. Our results show that this simple but effective modification improves the performance of the state-of-the-art in several different metrics for evaluating GANs: GAN-Train, GAN-Test, FID, Average Confidence Score etc. (see Section 4.4). Moreover, we show that augmenting downstream classification task using the images generated from the proposed method improves its robustness to noisy labels (Figure 3).

Our contributions can be summarized as:

- to our knowledge, we are the first to propose additive angular loss with margin for conditional GAN setting, bringing the recent success of angular margin losses from supervised discriminator models to conditional GANs
- we improve state-of-the-art labeled conditional GANs in recently proposed metrics of GAN-test and GAN-train, particularly improving the performance of downstream tasks when using generated images for augmentation,
- show that learning representation that increases intra-class compactness and inter-class separation can improve robustness to label noise.

## 2. Related Work

### Multi-domain image-to-image translation with cGAN:

Conditioning GANs has been an active research field ever since Mirza *et al.* [29] first showed that auxiliary information such as target label can be fed into standard GANs [12] to generate images conditioned on the auxiliary information. Various forms of representations such as one-hot encoded target domain label [6, 8, 17, 25, 51], source domain in the form of semantic text or layout representa-

tions [37, 49, 18, 52], source information in the form of images [20, 19, 26], geometry captured in the form of sparse landmarks [48] have successfully been applied to control the nature of synthetic data. Popular image-to-image translation works such as [20, 22] generate visually pleasing images, and may use reconstruction loss such as cycle consistency to preserve the major attributes of the source image [54]. However, these methods still lack enough control over target class and do not have explicit constraint to generate images having high fidelity to target classes.

In order to improve the fidelity of the target attributes in synthetic images, in addition to conditioning the network with one-hot target vector, AC-GAN [32] first proposed adding an auxiliary classification loss to the discriminator. Recent works have unified the ideas of standard adversarial loss, reconstruction loss and auxiliary classification loss to develop powerful class labeled image-to-image translation GANs with better control over target domains [17, 8, 25, 4, 10].

**Improving GAN Discriminator:** The well known stability and convergence problems of GANs have led to several contributions towards better behaved GAN objective [1], regularization on weights and normalization [13, 28, 30, 33], consistency based regularization [5, 50], or modifying the discriminator to learn more powerful representations [39] and be robust against adversarial attacks [53]. The importance of discriminator is further reinforced by several recent contributions in conditional GAN settings as well. Apart from [31], who propose combining class vector information via inner product in discriminator instead of commonly used concatenation, most other recent work propose adding extra regularization loss or modifying the discriminator task including auxiliary classifiers. TAC-GAN [11] propose an extra classifier to add negative class conditional entropy term to AC-GAN to improve the density of generated samples near decision boundary of the classifier, while [14] propose using mutual information between generated data and labels instead of adding the classifier.

### Rethinking soft-max classification cross-entropy loss:

The standard soft-max cross-entropy loss for auxiliary classifier do not explicitly take into account the relationship between data samples. Center loss [45] imposes the intra-class compactness but does not increase the inter-class separation. Contrastive loss [42] brings the similar points together and pushes the dissimilar ones, but it requires the paired or triplet examples. Angular loss with margin has shown state-of-the-art results in supervised discriminative models while promoting intra-class compactness and inter-class separation, and leveraging the intrinsic angular distribution of deep features [44, 9, 7]. We build on this development

Metric \ $\lambda_{cls}$	0.5	1.0 (default)	1.5	2	5	10
GAN-train $\uparrow$	22.0	23.0	17.0	14.0	13.0	10.0
GAN-test $\uparrow$	53.0	58.0	65.0	58.0	46.0	39.0
FID $\downarrow$	58.0	66.7	108.9	110.3	117.4	133.9

Table 1. Performance of baseline method with varying weight of class cross-entropy loss on Discriminator on CIFAR-100

and replace soft-max with additive angular margin loss (AAM) [9] in the auxiliary classifier of conditional GAN framework. We show that increasing intra-class compactness and inter-class separation by using AAM loss helps generator to synthesize images with high class fidelity and coverage, and improving the performance of downstream tasks when used for augmentation. Concurrent works reinforce the potential of this direction to learn representation leveraging inductive bias about the relationship of data samples: *the Rumi framework* in [2] learns a discriminator to classify images into positive-class real, negative-class-real and fake images, and [21] use conditional contrastive loss to increase intra-class compactness and inter-class separation. Our method is simple but effective that can be adapted to any auxiliary classifier based GANs.

### 3. Method

This section introduces class labeled conditional GAN followed by our proposed modification in discriminator with additive angular margin (AAM) loss.

#### 3.1. Class labeled conditional GAN

In class labeled conditional GAN, given an input image  $x$  and target category information  $c$ , the objective is to translate  $x$  faithfully to a new image  $x^c$  of the target category. We consider the case where  $c$  is prescribed using one-hot vector representation, the discriminator  $D$  is equipped with a separate branch for auxiliary classifiers, and a single generator  $G$  is trained to generate images of multiple categories, i.e.  $x^c = G(x, c)$  (see Figure 1).

Let us consider a labeled training dataset,  $\mathcal{D} = \{(x_i, y_i) \mid i = 1, 2, \dots, N\}$ , where  $x_i \in \mathbb{R}^{W \times H \times 3}$  is an input image of width  $W$  and height  $H$  of category  $y_i \in \mathbb{R}^C$  represented as one-hot encoded vector.  $C$  and  $N$  are the number of categories and total images in the training set respectively. Discriminator  $D$  estimates probability distribution over images with  $D_{src}(x)$  giving probability that  $x$  is real, and over category labels with  $D_{cls}(y|x)$  giving probability that  $x$  belongs to category  $y$ . The goal is to use this  $D$  in GAN framework such that the images generated by generator  $G$ ,  $x^c = G(x, c)$  follows the unknown true distribution  $P(x^c|c)$  while preserving remaining attributes of  $x$ . Training the network depends on three loss components described below.

**Adversarial Loss** This is similar to the standard unsupervised loss where  $D$  learns to identify real vs fake images,

and  $G$  learns to fool  $D$  by producing realistic images. As this is a conditional image-to-image translation GAN, one difference from general GANs is that the generator takes as input a source image  $x$  and target class  $c$ .

$$\mathcal{L}_{adv} = \mathbb{E}_x [\log D_{src}(x)] + \mathbb{E}_{x,c} [\log (1 - D_{src}(G(x, c)))], \quad (1)$$

**Reconstruction Loss** In order to preserve the content of the source image  $x$  that are not relevant or invariant to target class  $c$ , we add a cycle consistency loss where  $G$  is encouraged to successfully synthesize back  $x$  when  $x^c = G(x, c)$  is fed as source image to  $G$  together with the original label  $y$ .

$$\mathcal{L}_{rec} = \mathbb{E}_{x,c,y} [\|x - G(G(x, c), y)\|_1], \quad (2)$$

**Discriminator Classifier Loss** In order to encourage preservation of target category, two losses corresponding to real images and fake images are incorporated. When using the real labeled data  $(x, y)$ ,  $D$  is trained to minimize the classification loss

$$\mathcal{L}_{cls}^r = \mathbb{E}_{x,y} [-\log D_{cls}(y|x)], \quad (3)$$

and we use synthetic or fake images to train  $G$  with

$$\mathcal{L}_{cls}^f = \mathbb{E}_{x,c} [-\log D_{cls}(c|G(x, c))]. \quad (4)$$

The classification loss  $\log D_{cls}(y|x)$  and  $\log D_{cls}(c|G(x, c))$  in previous works use soft-max cross entropy loss, which we propose to replace with a new angular loss with margin (see Section 3.2).

**Combined Loss** The three losses are combined to train conditional GAN in a minmax game where we train  $D$  by minimizing

$$\mathcal{L}_D = -\mathcal{L}_{adv} + \lambda_{cls} \mathcal{L}_{cls}^r, \quad (5)$$

and train  $G$  by maximizing

$$\mathcal{L}_G = \mathcal{L}_{adv} + \lambda_{cls} \mathcal{L}_{cls}^f + \lambda_{rec} \mathcal{L}_{rec}. \quad (6)$$

While several works improved training stability and realism of synthetic images by modifying Discriminator with regards to the adversarial loss component [1, 13, 30, 33], few concurrent works have started exploring to improve conditional GAN by modifying auxiliary loss component [11, 14, 21]. We focus on improving this aspect of the GAN training.

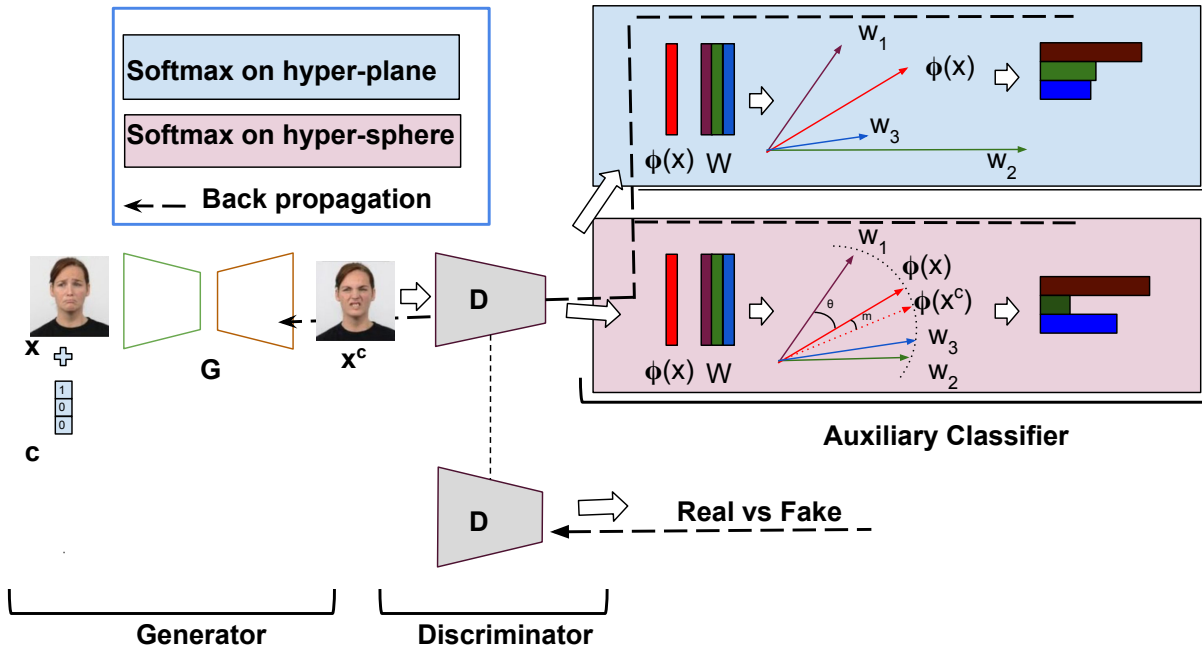


Figure 1. Overall pipeline of Modified Discriminator Classification Loss. We modified the original Softmax loss (right-top) in Auxiliary classifier by introducing an additive angular margin ( $m$ ) on its hyper-sphere projection (right-bottom).

### 3.2. Angular Attributes Classification Loss

As seen in Table 1, the auxiliary classification loss plays an important role in generating higher quality samples. The gradients from the auxiliary loss are used not just in training  $D$  but propagate to  $G$  as well when maximizing  $G$ 's objective in Equation 6 (also see Figure 1). Most of the existing labeled conditional GAN including AC-GAN, StarGAN, STGAN, AttGAN use the soft-max classifier with cross-entropy loss function for  $D_{cls}$  in Equations 3 and 4 given by,

$$L_s = -\frac{1}{N} \sum_{i=1}^N \log \frac{e^{W_{y_i}^T \phi(x_i) + b_{y_i}}}{\sum_{j=1}^C e^{W_j^T \phi(x_i) + b_j}} \quad (7)$$

where  $\phi(x_i) \in \mathbb{R}^d$  denotes the deep feature of the input sample  $x_i$  having class label  $y_i$ .  $W \in \mathbb{R}^{d \times C}$  is the weight matrix where  $C$  is the number of classes,  $W_j \in \mathbb{R}^d$  the weight vector in column  $j$  and  $b_j \in \mathbb{R}^n$  the bias vector. We propose to make the auxiliary classifier more powerful by taking advantage of the intrinsic angular distribution of the deep features, and to learn the representation that increases both the intra-class compactness and inter-class separation. We set the bias vectors  $b_j$  to 0, normalize the weight vectors  $W_j$  to unit magnitude, and normalize deep feature vector  $\phi(x_i)$  to unit magnitude and scale it by  $s$ . Thus, the feature embeddings are distributed in a hypersphere of radius  $s$  and the output predictions are dependent only on the

angle between the weight vectors and feature vector given by  $\theta_j = \arccos(W_j^T \phi(x_i))$ . As shown in Figure 1, this makes the embedding features to be distributed around a center of the surface area representing each category. In order to improve the intra-class compactness and inter-class separation, we add an additional angular margin  $m$  between  $x_i$  and  $W_{y_i}$ . This leads to the modification of the standard soft-max cross entropy loss in Equation 7 to additive angular margin (AAM) loss given by,

$$L_{ang} = -\frac{1}{N} \sum_{i=1}^N \log \frac{e^{s(\cos(\theta_{y_i} + m))}}{e^{s(\cos(\theta_{y_i} + m))} + \sum_{j=1, j \neq y_i}^C e^{s \cos \theta_j}} \quad (8)$$

We use this modified AAM loss in the auxiliary classification component of the discriminator  $D_{cls}$  in Equations 3 and 4.

## 4. Experiments

### 4.1. Dataset

We evaluate the proposed method on two different datasets: facial expression images, **RaFD** [24], and natural images with 100 classes, **CIFAR-100** [23]. We chose these datasets with distinct characteristics to validate that we can benefit from the angular distribution of deep features of natural images in different settings, and that the proposed method is not limited to specific data domain. **RaFD** con-



sists of 8040 face images annotated with eight different facial expressions. We split the dataset into two equal halves as training and test sets. The images are aligned based on their landmarks and cropped to the size of  $128 \times 128$ . **CIFAR-100** is a challenging dataset for natural image classification problem consisting of 50K training and 10K test examples from 100 different classes. Another reason to choose this dataset is that it has sufficiently large number of classes while not being too big such that the experiments can be run with reasonable computational resources.

## 4.2. Implementation Details

We implemented our algorithms on PyTorch. The experiments were carried out in a machine with an i7 processor and Titan 1070 Geforce GPU in Ubuntu Operating System. We train our model for 200K iterations. While training we set the initial learning rate as of 0.0001 for both Generator and Discriminator. The learning rate is decayed after every 10K iterations. Please check our code in the supplementary for the further implementation details. We make our code public upon the acceptance of the paper.

## 4.3. Compared Methods

We compared our method with several other class conditional GAN baselines from both the natural image domain and facial image domain. Methods such as SNGAN [30], WGAN-GP [13], DCGAN [35], PixelCNN++ [38] are extensively evaluated on natural image domain. Similarly, StarGAN [8], EF-GAN [46], Ganimation [34] are mostly evaluated on face benchmarks. We compared our method with these methods either quantitatively or qualitatively or both. Among these baselines, StarGAN is the closest one as its architecture is designed to directly address the problem of target label retention on synthetic examples. Other comparable architectures are AttGAN [17], STGAN [25]. Recent extensive comparative study [4] on the performance of StarGAN, AttGAN, STGAN on different conditioning methods identified similar trends on these architectures. Thus, we expect similar impact of our method on AttGAN and STGAN as in StarGAN, and hence use StarGAN as the baseline for most of the comparisons in this work.

EF-GAN and Ganimation are not directly comparable. EF-GAN trains multiple number of local GANs along with a global GAN in an hierarchical fashion. Whereas, Ganimation uses semantic masks as an extra information. Our method does not need any extra parameters. Other indirectly comparable methods are SNGAN, WGAN-GP as they do not directly address the problem of preserving labels on synthetic data directly, and focus on bringing stability in training with regularization in discriminator weights. Thus, these are complementary to our methods and their impact on the proposed method may be assessed independently. While this is an interesting direction, it is beyond

Method	GAN-Train $\uparrow$	GAN-Test $\uparrow$
SNGAN [30]	45.0	59.4
WGAN-GP(10M) [13]	26.7	40.4
WGAN-GP(2.5M) [13]	5.4	4.3
DCGAN [35]	3.5	2.4
PixelCNN++ [38]	4.8	27.5
StarGAN [8]	23.0	58.3
Ours	30.0 (+7.0)	71.8 (+13.5)

Table 2. Comparison of GAN-Train and GAN-Test on CIFAR-100. We compared our method with some of the recent GAN architectures extensively evaluated on natural image generation. We use average image class recognition rate to measure the performance. Our method obtains highest and the second-highest performance on GAN-Test and GAN-Train respectively.

Method	GAN-Train $\uparrow$	GAN-Test $\uparrow$
Ganimation [34]	84.36	\
EF-GAN [46]	89.38	\
StarGAN [8]	91.33	89.85
Ours	93.2 (+1.87)	95.16 (+5.31)

Table 3. Comparison of GAN-Train and GAN-Test on RaFD dataset. We use average attribute recognition rate to compare the performance of our method with three state-of-the-art methods for expressions translation. Our results show highest performance on both GAN-Train (vs.all three) and GAN-Test (vs. StarGAN).

the scope of current work. TAC-GAN [11] and Projection Discriminator [31] tackle the problem similar to ours. However, TAC-GAN demands extra learnable parameters equal to that of a discriminator. Projection Discriminator [31] injects label information to intermediate layers and learn the parameters in adversarial fashion without using an auxiliary loss. Our focus is on improving the auxiliary classifier component of the GAN. Even then, we have compared with some of the representative works from this category see where our method stands in terms of performance with contemporary approaches.

## 4.4. Quantitative Evaluation

**GAN-Train and GAN-Test:** These are recently proposed metrics to evaluate the performance of GANs [40]. In GAN-train, a classifier is trained using synthetic images as input and the target labels used to generate corresponding images as ground truth label. GAN-train is this classifier’s prediction score on real test set. Similarly, GAN-test is the prediction score of a classifier on a synthetic test set when the classifier is trained using a real images. This is equivalent to attribute generation rate calculated on the recent labeled conditional GANs [25, 4].

To evaluate GAN-Test on CIFAR-100, we train ResNet-18 [15] on CIFAR-100 train set. The performance of this model on CIFAR-100 test set is 77%. Table 2 shows the performance comparison of the proposed method with several directly and indirectly comparable contemporary meth-

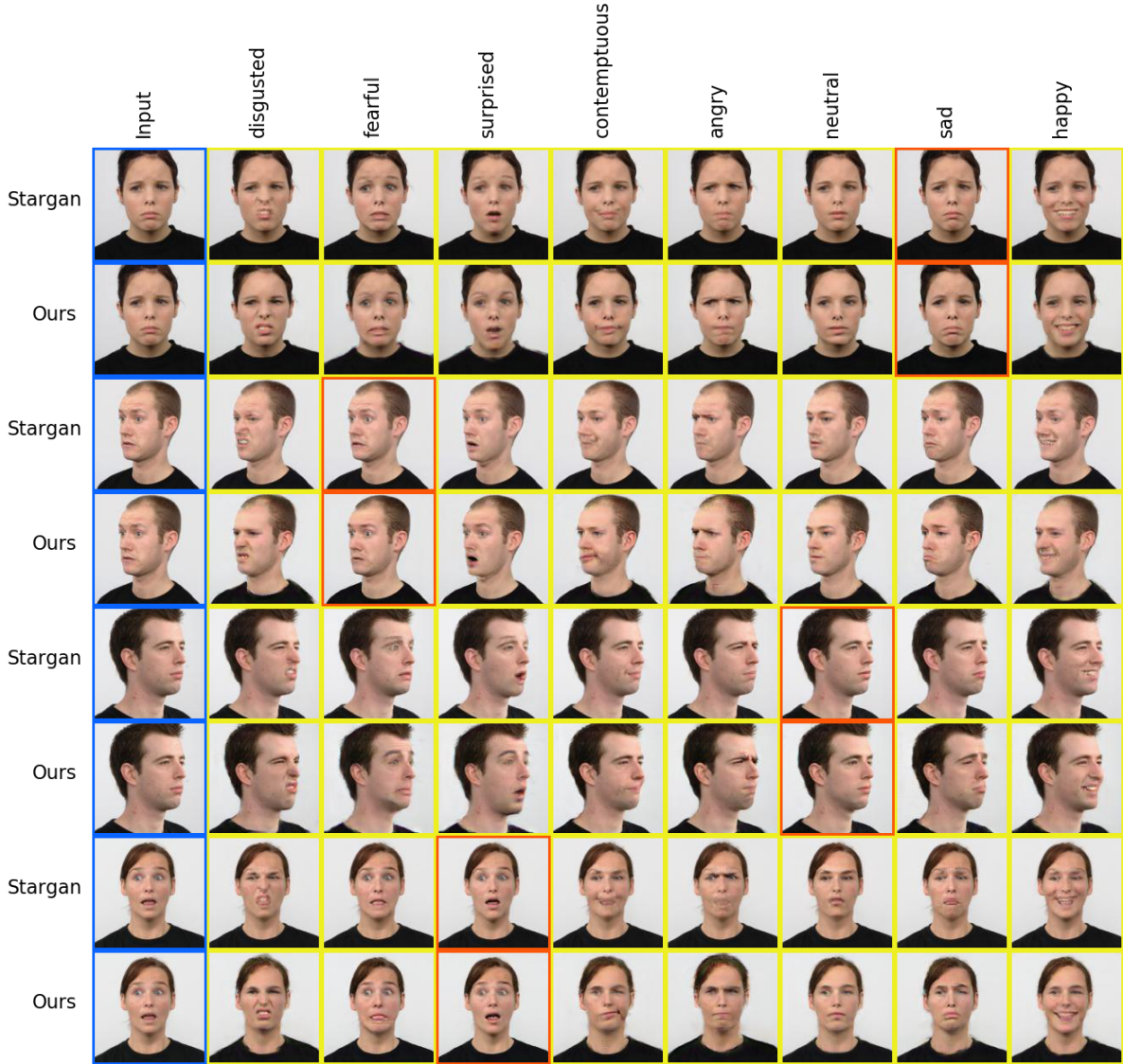


Figure 2. Qualitative comparison of face expression translation on RaFD dataset. Here, first column (blue) shows the input image, red border shows the reconstruction and the rest of the column (yellow) shows its translated images. Label in each column starting from second column encodes the target attribute. Label on the rows are the applied methods. From these qualitative comparison, we see less artifacts and better preservation of the target attributes.

ods for CIFAR-100. As we see in the table, our method makes a substantial improvement over the baseline by +7% on GAN-train and +13.5% on GAN-test. Also, our method outperforms almost every compared method in both the metrics, next to SNGAN in GAN-Train. As mentioned before, SNGAN focuses in improving discriminator by regularizing every layer without a particular focus on auxiliary classification for class retention problem. Combining such regularization approach of SNGAN with our method may further improve the performance, and is left as future work. Performance of most of the methods are in lower band due to highly challenging in nature of CIFAR-100. Since the

GAN-train and GAN-test are akin to two competing metrics of precision and recall, consistent performance on both the metrics validates that the proposed method is effective in handling a data set with large number of classes.

Similarly, Table 3 shows the performance comparison on RaFD. Our approach surpasses the performance of the StarGAN by +1.87% on GAN-train and +13.5% on GAN-test. In addition to this, our method also outperforms Ganimation and EF-GAN which are state-of-the-art methods in performing conditional GANs for expressions translation. This consistency in performance across two contrasting nature of benchmarks clearly validates the benefit of the proposed

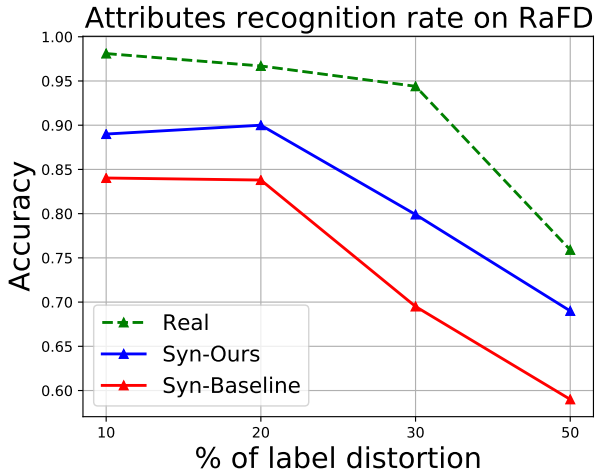


Figure 3. Comparison of attribute recognition rate on GAN-synthetic data by the model trained with different proportion of labels distorted. The distortion on label makes the classifier weak. This evaluates how robust are the labels on the synthetic data. Syn-Ours is the performance of our method. Whereas, Syn-Baseline is the performance of StarGAN.

Dataset	Method	FID (Backbone) ↓
RaFD	Ganimation [34]	45.55 (Inception V4)
RaFD	EF-GAN [46]	42.36 (Inception V4)
RaFD	StarGAN [8]	6.14 (Inception V3)
RaFD	Ours	5.35 (Inception V3)
RaFD	StarGAN [8]	7.89 (Inception V4)
RaFD	Ours	6.17 (Inception V4)
CIFAR-100	StarGAN [8]	66.74 (Inception V3)
CIFAR-100	Ours	53.73 (Inception V3)

Table 4. FID comparison on both CIFAR-100 and RaFD. We computed the FID taking both InceptionV3 and InceptionV4 as backbone. Our method outperforms these competitive baselines.

method. It also shows that the proposed angular geometric constraint is better at capturing the underlying distribution of data independent to the choice of particular image dataset benchmark.

**Performance on weak classifier:** We compare GAN-test score further using a weak classifier which is trained on real data with different proportion of labels distorted. Figure 3 shows that the performance on classifiers trained with noisy label is better when using proposed method compared to the baseline of StarGAN.

**Fréchet Inception Distance (FID):** FID [43] is a widely used metric that measures the similarity of synthetic image statistics to the real image statistics using features of real and fake images. Lower FID values correspond to better quality of fake images of GAN evaluation that measures Table 4 shows the FID comparison on both RAFD and CIFAR-100. On both the benchmarks our method improves performance

over the baseline which shows that imposing angular distribution geometry constraint in order to faithfully retain the target label on translated images does not hurt the other quality metric.

**Data Augmentation:** This approach evaluates the benefit of adding synthetic images as part of data augmentation when training a classifier model with a real training data. The evaluation metric measures the attribute classification performance of a model on a real test set, where the model is trained using real data and data augmentation with synthetic data.

Table 5 reports the performance comparison on data augmentation using average attribute classification accuracy on real test examples of CIFAR-100. We followed the experimental setup proposed in [41] to evaluate the performance. *Real only!* are the numbers reported in [41] and *Real only* are the results obtained in our implementation which are slightly lower but still comparable. We augmented the variable size of real training examples 2.5K, 5K and 10K with 50K of synthetic data obtained from StarGAN and our method. The table reports the performance of a classification model trained on each of these combinations of real and synthetic data. We can see that the classifier trained on the data augmented with our synthetic data clearly outperforms the model trained on the data augmented with StarGAN. The interesting point to note here is, when the real data set size is 10K, augmenting StarGAN synthetic data with real data gives lower performance in comparison using only real data. The performance using our synthetic example is still higher than using only real images, providing evidence that our method is able to translate more faithfully the images with better preserved target label. However, it is still an open problem to improve by large margin the performance of discriminative model using data augmentation from synthetic example when very large number of real examples are available.

**Average confidence score:** This is another recently proposed metric [27] as attribute preserving for conditional GAN. Here, class conditional probability on GAN-test examples are evaluated by a model trained on real training examples. We trained a preactivation variant ResNet-18 [16] on CIFAR-100 (just mentioned before) and applied on 100K GAN-synthetic data. Figure 6 compares the confidence score distribution of GAN synthetic test examples. Ideally, all the mass should concentrate on right side (confidence 1) and make a single pole. In practice, our method has higher mass on right side than the StarGAN. This demonstrates that our method generates images more faithfully and confidently. It can be argued that generating an easy example may improve such metric. However, performance



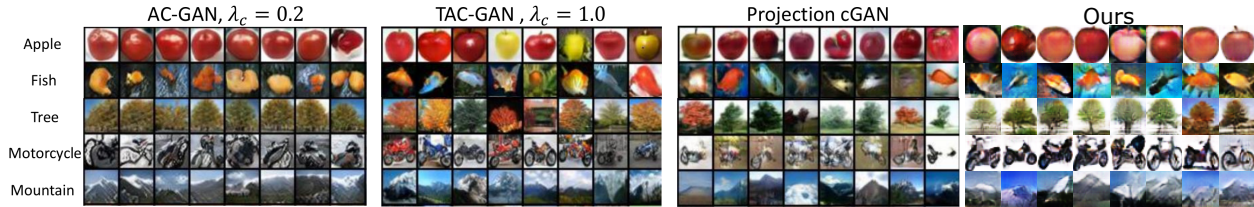


Figure 4. Here we make qualitative comparison of some of the recent methods with our proposed method. These are the randomly sampled images from five different categories. From these synthetic examples, we can clearly see our method generating images with lesser noise, better contrast and diversities too. If we carefully observe the shape of the apples, we can see the shape of the apples are distorted by all the existing methods. Whereas, our method managed to preserved its shape well.

Setup \ Real data size(K)	2.5	5.0	10.0
Real only! [40]	25.6	40.0	51.5
Real only	24.39	36.32	51.13
Real + Syn (Stargan, 50K)	31.45 (+7.06)	39.65 (+3.3)	49.22 (-1.91)
Real + Syn (Ours, 50K)	37.25 (+12.86)	44.20 (+7.98)	51.83 (+0.7)

Table 5. Performance comparison of data augmentation on CIFAR-100 using average attribute classification accuracy (higher is better). We followed the experiment setup proposed in [40]. Real only! are the numbers reported by them, whereas Real only are from our implementation. We augmented 50K synthetic data with the variable size of real training examples shown in the top row.

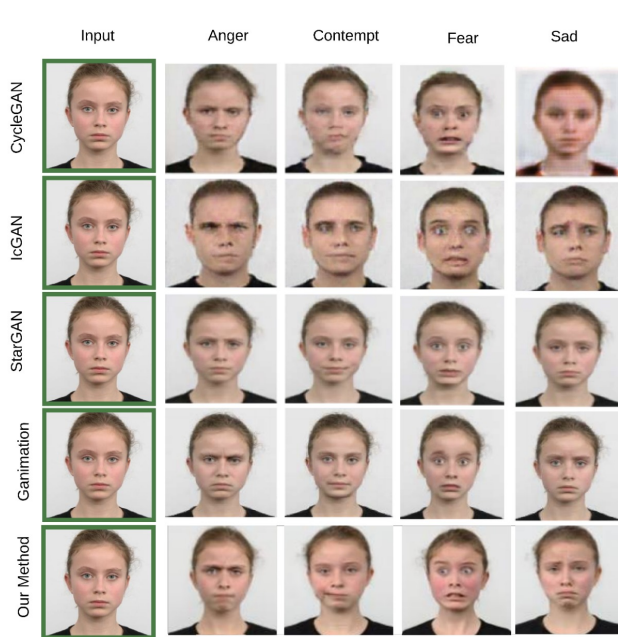


Figure 5. Qualitative comparison of attribute translation on RaFD. In comparison to the previous methods, our translations are more intense with less artifacts and better contrast.

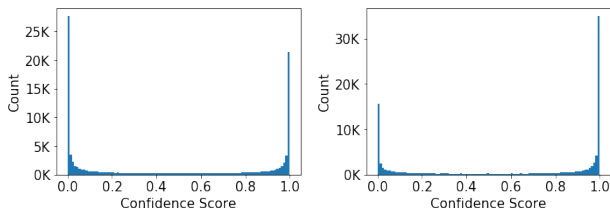


Figure 6. Distribution of confidence scores on GAN synthetic image on CIFAR-100 : StarGAN (Left) and Ours (Right).

of our method on other metrics such as GAN-train, FID easily refutes it.

**Qualitative Evaluations** For qualitative evaluations on CIFAR-100, please refer Figure 4 with inline explanation on caption. Similarly, we present qualitative comparisons with Ganimation, StarGAN, CycleGAN on RaFD in Figure 14. Similarly, find additional qualitative comparisons on RaFD in Figure 2.

## 5. Conclusion

The proposed AAM loss in auxiliary classifier of labeled conditional GANs with its nice geometrical properties help synthesize high fidelity target class which is an important problem in face data applications. Some recent methods like TAC-GAN [11] and UAC-GAN [14] use extra constraint to prevent generator generate only “easy” samples for the auxiliary classifier away from its decision boundary. We believe that the issue may be less severe with our proposed method where we make the classifier stronger and map the real images into a manifold with high intra-class compactness and large margin to separate inter-class samples. Several experiments and evaluation metrics show that this geometry aware loss leading to better representation helps generator synthesize higher quality images preserving better the target labels. While better representation learning with inductive bias on the manifold of conditional data distribution looks promising, it is still an open problem to completely understand the dynamics of conditional GAN training, where generator and discriminators equipped with classifiers compete in the non-stationary environment, and have complex interaction between learned representation

of each network component and the various regularization constraints added to the system for training stability. Detailed analysis of all these components with ablation studies to understand their impact would be an interesting future direction to pursue.

## References

- [1] Martin Arjovsky, Soumith Chintala, and Léon Bottou. Wasserstein gan. *arXiv preprint arXiv:1701.07875*, 2017. [2](#), [3](#)
- [2] Siddarth Asokan and Chandra Seelamantula. Teaching a gan what not to learn. In *NeurIPS*, volume 33, 2020. [3](#)
- [3] Binod Bhattarai, Seungryul Baek, Rumeysa Bodur, and Tae-Kyun Kim. Sampling strategies for gan synthetic data. In *ICASSP*, 2020. [1](#)
- [4] Binod Bhattarai and Tae-Kyun Kim. Inducing optimal attribute representations for conditional gans. In *ECCV*, 2020. [2](#), [5](#)
- [5] Ting Chen, Xiaohua Zhai, Marvin Ritter, Mario Lucic, and Neil Houlsby. Self-supervised gans via auxiliary rotation loss. In *CVPR*, 2019. [2](#)
- [6] Xi Chen, Yan Duan, Rein Houthoofd, John Schulman, Ilya Sutskever, and Pieter Abbeel. Infogan: Interpretable representation learning by information maximizing generative adversarial nets. In *NIPS*, 2016. [2](#)
- [7] Hongjun Choi, Anirudh Som, and Pavan Turaga. Amc-loss: Angular margin contrastive loss for improved explainability in image classification. In *CVPRW*, 2020. [2](#)
- [8] Y. Choi, M. Choi, M. Kim, J-W. Ha, S. Kim, and J. Choo. StarGAN: Unified generative adversarial networks for multi-domain image-to-image translation. In *CVPR*, 2018. [1](#), [2](#), [5](#), [7](#)
- [9] Jiankang Deng, Jia Guo, Niannan Xue, and Stefanos Zafeiriou. Arcface: Additive angular margin loss for deep face recognition. In *CVPR*, 2019. [2](#), [3](#)
- [10] Baris Gecer, Binod Bhattarai, Josef Kittler, and Tae-Kyun Kim. Semi-supervised adversarial learning to generate photorealistic face images of new identities from 3d morphable model. In *ECCV*, 2018. [1](#), [2](#)
- [11] Mingming Gong, Yanwu Xu, Chunyuan Li, Kun Zhang, and Kayhan Batmanghelich. Twin auxiliary classifiers gan. In *NeurIPS*, 2019. [2](#), [3](#), [5](#), [8](#)
- [12] Ian Goodfellow, Jean Pouget-Abadie, Mehdi Mirza, Bing Xu, David Warde-Farley, Sherjil Ozair, Aaron Courville, and Yoshua Bengio. Generative adversarial nets. In *NeurIPS*, 2014. [2](#)
- [13] Ishaan Gulrajani, Faruk Ahmed, Martin Arjovsky, Vincent Dumoulin, and Aaron C Courville. Improved training of wasserstein gans. In *NeurIPS*, 2017. [2](#), [3](#), [5](#)
- [14] Ligong Han, Anastasis Sathopoulos, Tao Xue, and Dimitris Metaxas. Unbiased auxiliary classifier gans with mine. In *CVPRW*, 2020. [2](#), [3](#), [8](#)
- [15] K. He, X. Zhang, S. Ren, and J. Sun. Deep residual learning for image recognition. In *CVPR*, 2016. [5](#)
- [16] Kaiming He, Xiangyu Zhang, Shaoqing Ren, and Jian Sun. Identity mappings in deep residual networks. In *ECCV*, 2016. [7](#)
- [17] Zhenliang He, Wangmeng Zuo, Meina Kan, Shiguang Shan, and Xilin Chen. Attgan: Facial attribute editing by only changing what you want. *IEEE TIP*, 2019. [1](#), [2](#), [5](#)
- [18] Seunghoon Hong, Dingdong Yang, Jongwook Choi, and Honglak Lee. Inferring semantic layout for hierarchical text-to-image synthesis. In *2018*, 2018. [2](#)
- [19] Xun Huang, Ming-Yu Liu, Serge Belongie, and Jan Kautz. Multimodal unsupervised image-to-image translation. In *ECCV*, 2018. [2](#)
- [20] Phillip Isola, Jun-Yan Zhu, Tinghui Zhou, and Alexei A Efros. Image-to-image translation with conditional adversarial networks. In *CVPR*, 2017. [1](#), [2](#)
- [21] Minguk Kang and Jaesik Park. Contragan: Contrastive learning for conditional image generation. In *NeurIPS*, volume 33, 2020. [3](#)
- [22] Tero Karras, Samuli Laine, and Timo Aila. A style-based generator architecture for generative adversarial networks. In *CVPR*, 2019. [1](#), [2](#)
- [23] Alex Krizhevsky, Geoffrey Hinton, et al. Learning multiple layers of features from tiny images. 2009. [4](#)
- [24] Oliver Langner, Ron Dotsch, Gijb Bert, Daniel HJ Wigboldus, Skyler T Hawk, and AD Van Knippenberg. Presentation and validation of the radboud faces database. In *Cognition and emotion*, 2010. [4](#)
- [25] Ming Liu, Yukang Ding, Min Xia, Xiao Liu, Errui Ding, Wangmeng Zuo, and Shilei Wen. Stgan: A unified selective transfer network for arbitrary image attribute editing. In *CVPR*, 2019. [2](#), [5](#)
- [26] Ming-Yu Liu, Thomas Breuel, and Jan Kautz. Unsupervised image-to-image translation networks. In *NeurIPS*, 2017. [2](#)
- [27] Rui Liu, Yu Liu, Xinyu Gong, Xiaogang Wang, and Hongsheng Li. Conditional adversarial generative flow for controllable image synthesis. In *CVPR*, 2019. [7](#)
- [28] Lars Mescheder, Andreas Geiger, and Sebastian Nowozin. Which training methods for gans do actually converge? In *ICML*, 2018. [2](#)
- [29] Mehdi Mirza and Simon Osindero. Conditional generative adversarial nets. *arXiv preprint arXiv:1411.1784*, 2014. [2](#)
- [30] Takeru Miyato, Toshiki Kataoka, Masanori Koyama, and Yuichi Yoshida. Spectral normalization for generative adversarial networks. In *ICLR*, 2018. [2](#), [3](#), [5](#)
- [31] Takeru Miyato and Masanori Koyama. cgans with projection discriminator. In *ICLR*, 2018. [2](#), [5](#)
- [32] Augustus Odena, Christopher Olah, and Jonathon Shlens. Conditional image synthesis with auxiliary classifier gans. In *ICML*, 2017. [1](#), [2](#)
- [33] Sung Woo Park and Junseok Kwon. Sphere generative adversarial network based on geometric moment matching. In *CVPR*, 2019. [2](#), [3](#)
- [34] Albert Pumarola, Antonio Agudo, Aleix M Martinez, Alberto Sanfeliu, and Francesc Moreno-Noguer. Ganimation: Anatomically-aware facial animation from a single image. In *ECCV*, 2018. [5](#), [7](#)
- [35] Alec Radford, Luke Metz, and Soumith Chintala. Unsupervised representation learning with deep convolutional generative adversarial networks. In *ICLR*, 2016. [5](#)



- [36] Suman Ravuri and Oriol Vinyals. Seeing is not necessarily believing: Limitations of biggans for data augmentation. In *ICLRW*, 2019. 1
- [37] Scott Reed, Zeynep Akata, Xinchen Yan, Lajanugen Logeswaran, Bernt Schiele, and Honglak Lee. Generative adversarial text to image synthesis. 2016. 2
- [38] Tim Salimans, Andrej Karpathy, Xi Chen, and Diederik P Kingma. Pixelcnn++: Improving the pixelcnn with discretized logistic mixture likelihood and other modifications. In *ICLR*, 2017. 5
- [39] Edgar Schonfeld, Bernt Schiele, and Anna Khoreva. A u-net based discriminator for generative adversarial networks. In *CVPR*, pages 8207–8216, 2020. 2
- [40] K. Shmelkov, C. Schmid, and K. Alahari. How good is my GAN? In *ECCV*, 2018. 1, 5, 8
- [41] Konstantin Shmelkov, Cordelia Schmid, and Karteek Alahari. How good is my gan? In *ECCV*, 2018. 7
- [42] Yi Sun, Xiaogang Wang, and Xiaoou Tang. Deep learning face representation from predicting 10,000 classes. In *CVPR*, 2014. 2
- [43] Thomas Unterthiner, Bernhard Nessler, Calvin Seward, Günter Klambauer, Martin Heusel, Hubert Ramsauer, and Sepp Hochreiter. Coulomb gans: Provably optimal nash equilibria via potential fields. *NeurIPS*, 2017. 7
- [44] Hao Wang, Yitong Wang, Zheng Zhou, Xing Ji, Dihong Gong, Jingchao Zhou, Zhifeng Li, and Wei Liu. Cosface: Large margin cosine loss for deep face recognition. In *CVPR*, 2018. 2
- [45] Yandong Wen, Kaipeng Zhang, Zhifeng Li, and Yu Qiao. A discriminative feature learning approach for deep face recognition. In *ECCV*, 2016. 2
- [46] Rongliang Wu, Gongjie Zhang, Shijian Lu, and Tao Chen. Cascade ef-gan: Progressive facial expression editing with local focuses. In *CVPR*, 2020. 5, 7
- [47] Yuan Xue, Jiarong Ye, Qianying Zhou, L Rodney Long, Sameer Antani, Zhiyun Xue, Carl Cornwell, Richard Zaino, Keith C Cheng, and Xiaolei Huang. Selective synthetic augmentation with histogan for improved histopathology image classification. *Medical Image Analysis*, 67:101816, 2020. 1
- [48] Egor Zakharov, Aliaksandra Shysheya, Egor Burkov, and Victor Lempitsky. Few-shot adversarial learning of realistic neural talking head models. *arXiv preprint arXiv:1905.08233*, 2019. 2
- [49] Han Zhang, Tao Xu, Hongsheng Li, Shaoting Zhang, Xiaogang Wang, Xiaolei Huang, and Dimitris N Metaxas. Stackgan: Text to photo-realistic image synthesis with stacked generative adversarial networks. In *CVPR*, 2017. 2
- [50] Han Zhang, Zizhao Zhang, Augustus Odena, and Honglak Lee. Consistency regularization for generative adversarial networks. In *ICLR*, 2020. 2
- [51] Zhifei Zhang, Yang Song, and Hairong Qi. Age progression/regression by conditional adversarial autoencoder. In *CVPR*, 2017. 2
- [52] Bo Zhao, Lili Meng, Weidong Yin, and Leonid Sigal. Image generation from layout. In *CVPR*, 2019. 2
- [53] Brady Zhou and Philipp Krähenbühl. Don’t let your discriminator be fooled. In *International Conference on Learning Representations*, 2019. 2
- [54] Jun-Yan Zhu, Taesung Park, Phillip Isola, and Alexei A Efros. Unpaired image-to-image translation using cycle-consistent adversarial networks. In *ICCV*, 2017. 1, 2



Figure 7. Qualitative comparison of attribute translation on RaFD. Blue boxed images are input and red boxed images are reconstructed images.



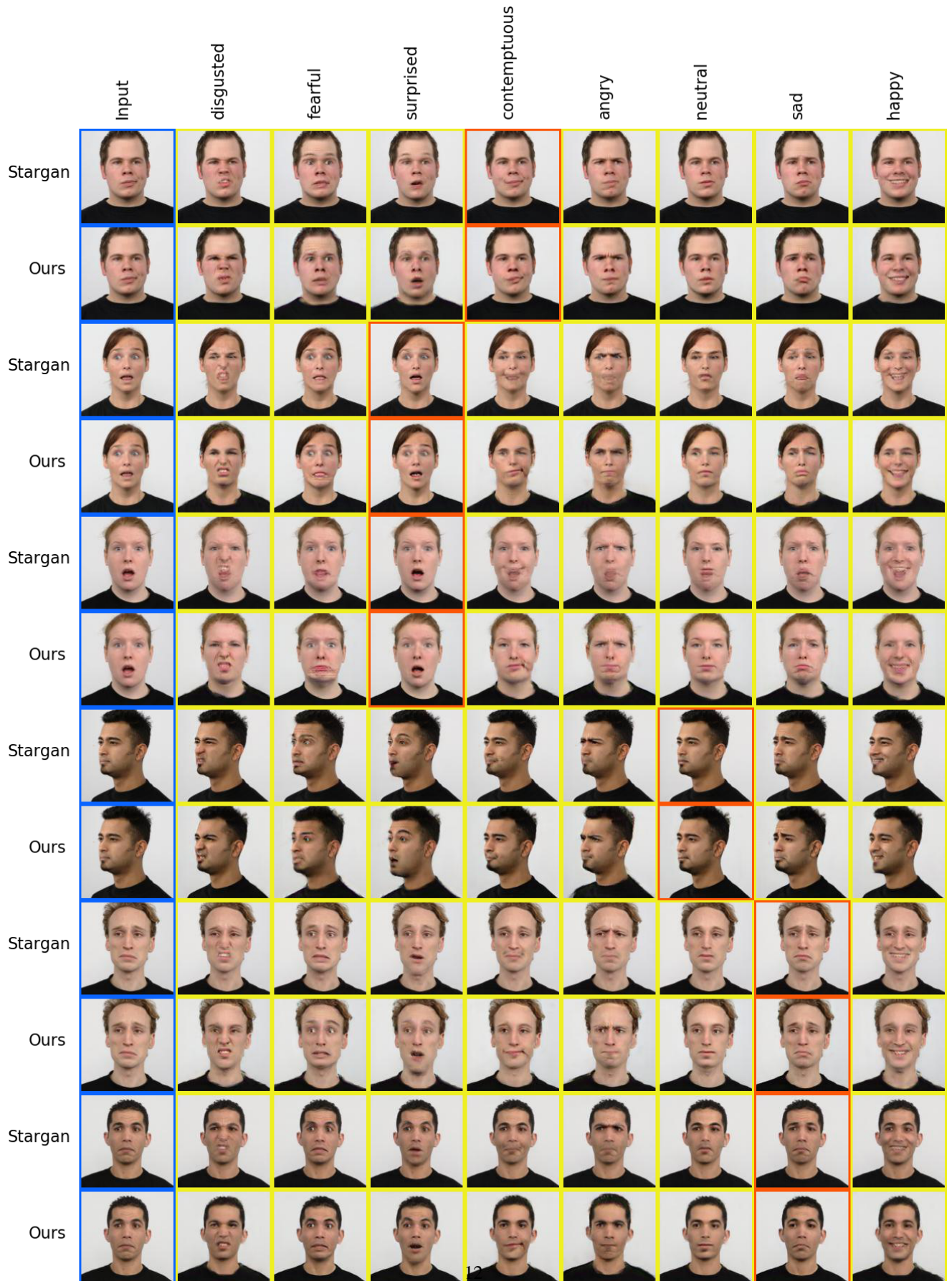


Figure 8. Qualitative comparison of attribute translation on RaFD. Blue boxed images are input and red boxed images are reconstructed images.

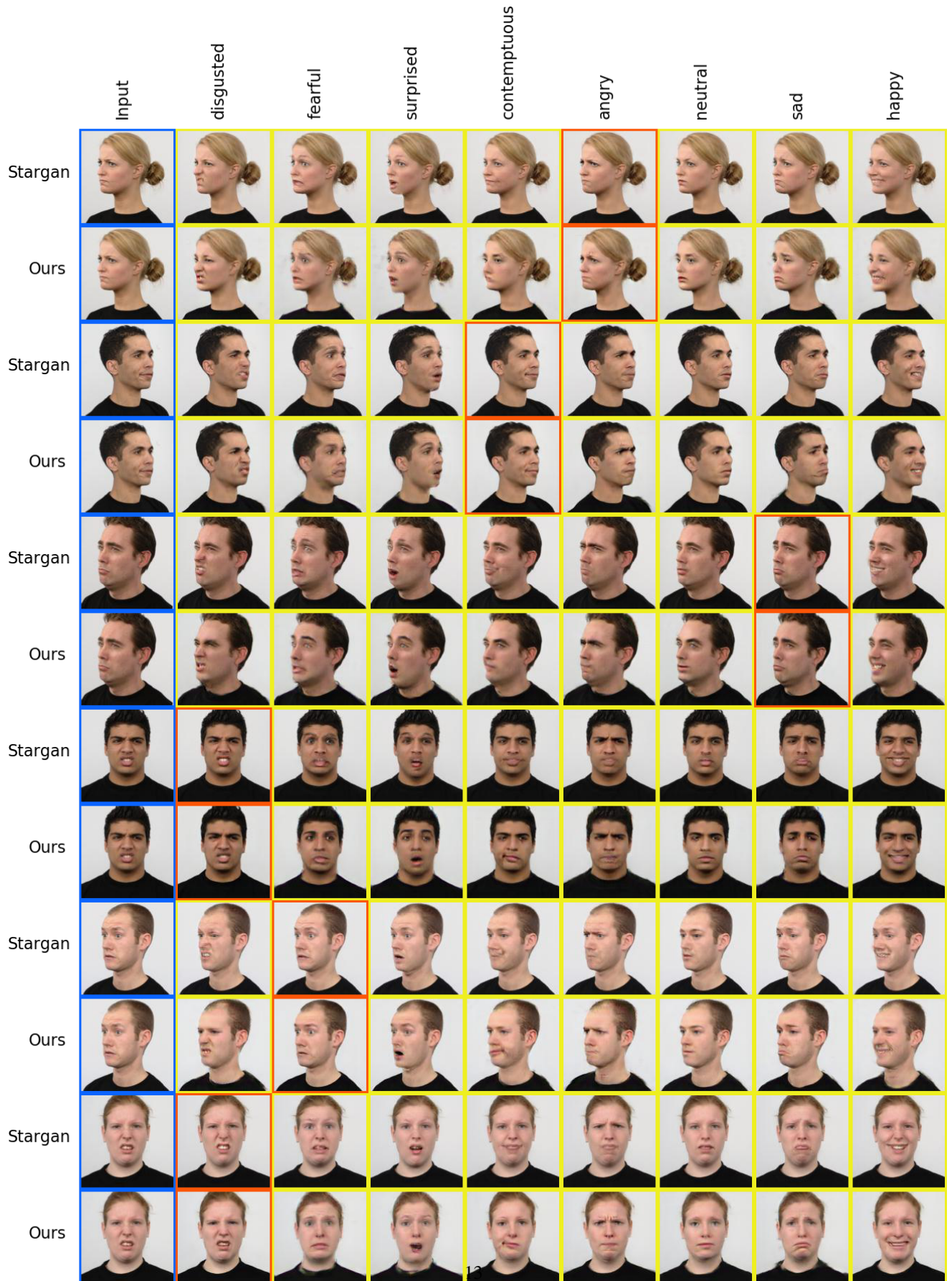


Figure 9. Qualitative comparison of attribute translation on RaFD. Blue boxed images are input and red boxed images are reconstructed images.





Figure 10. Qualitative comparison of attribute translation on RaFD. Blue boxed images are input and red boxed images are reconstructed images.



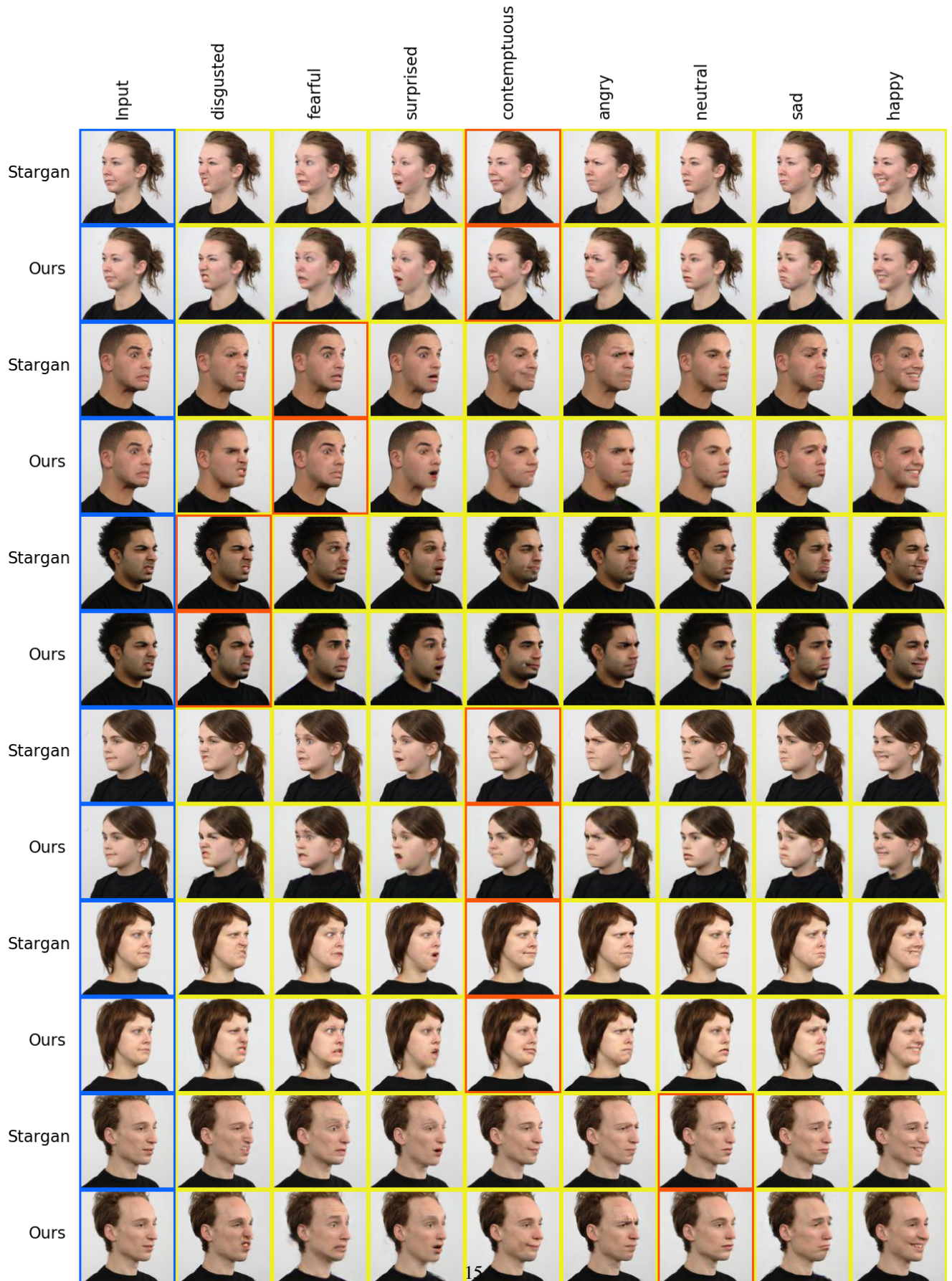


Figure 11. Qualitative comparison of attribute translation on RaFD. Blue boxed images are input and red boxed images are reconstructed images.

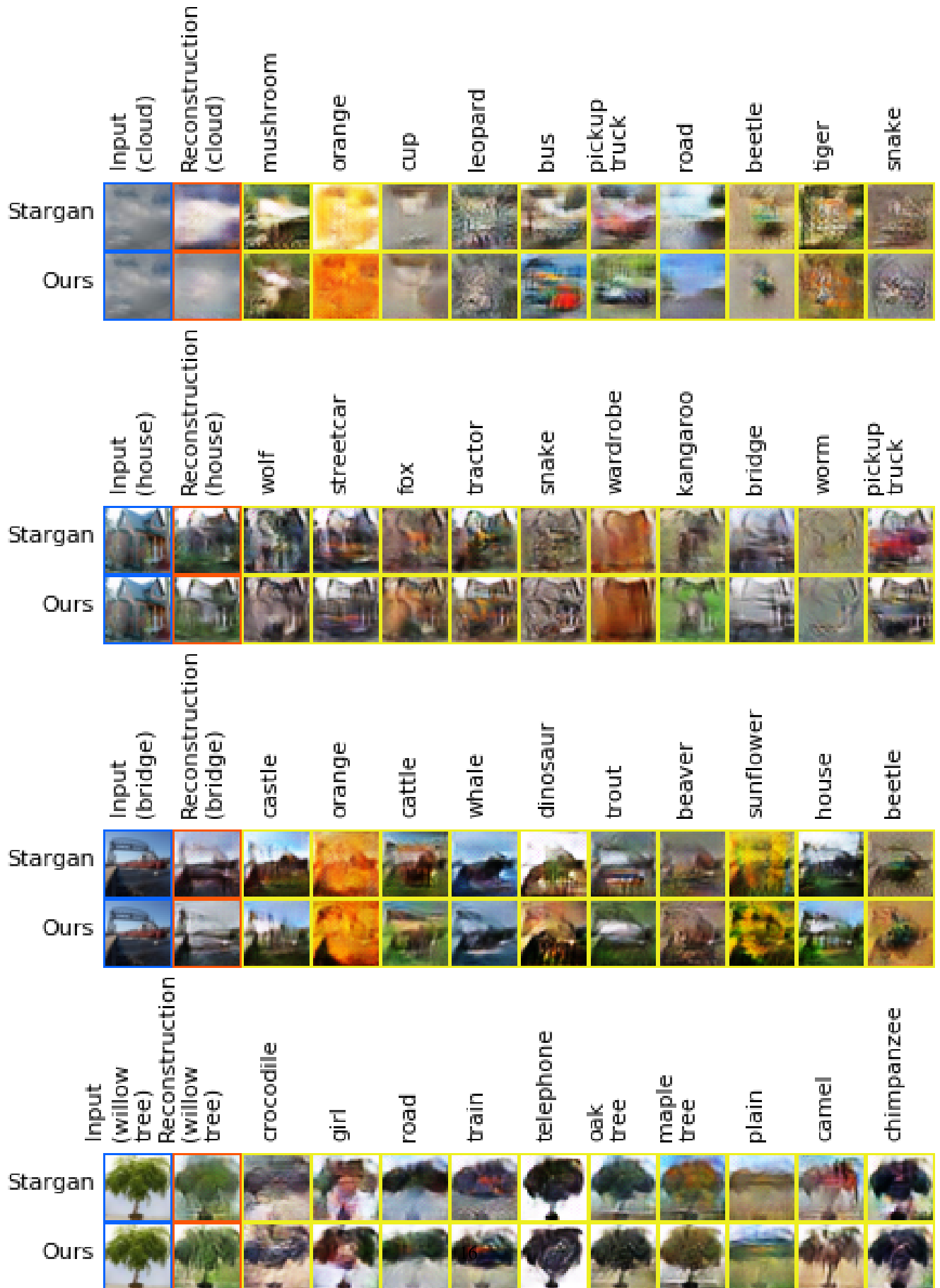


Figure 12. Qualitative comparison of category translation on CIFAR-100. Blue boxed images are input and red boxed images are reconstructed images.

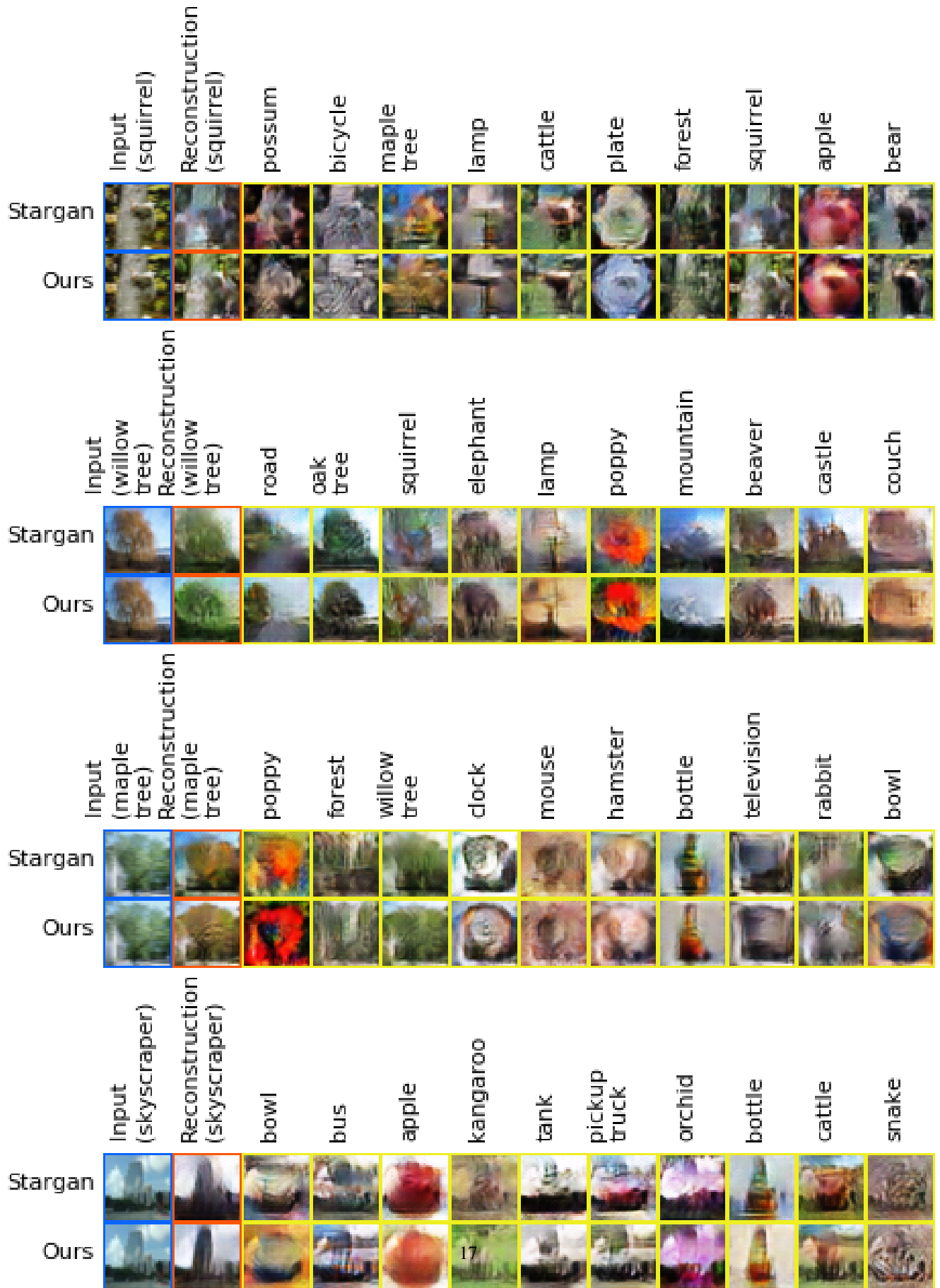


Figure 13. Qualitative comparison of category translation on CIFAR-100. Blue boxed images are input and red boxed images are reconstructed images.

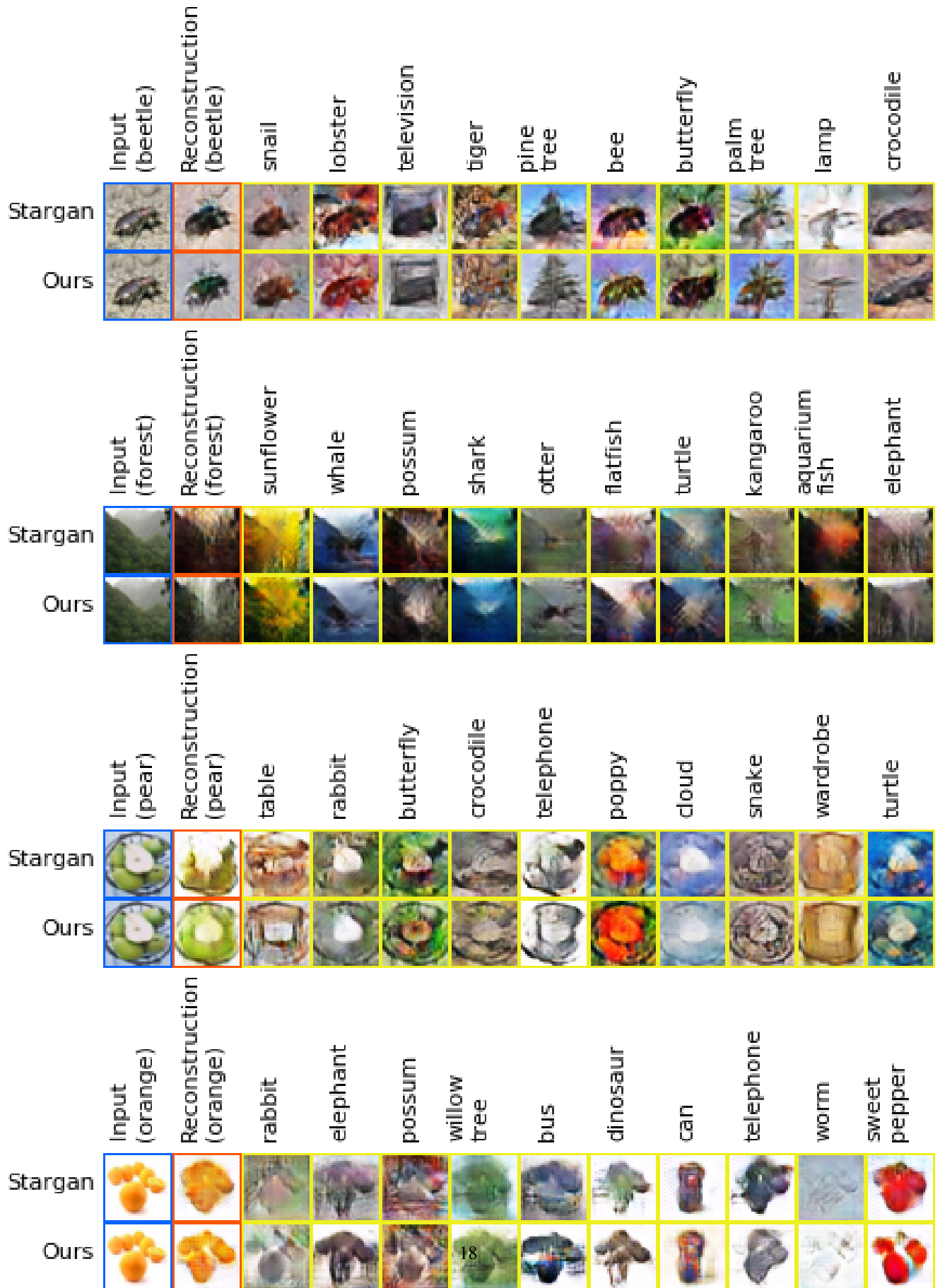


Figure 14. Qualitative comparison of category translation on CIFAR-100. Blue boxed images are input and red boxed images are reconstructed images.